Aaron Knobloch[1]
Fellow ASME
General Electric Global Research,
KWB322,
One Research Circle,
Niskayuna, NY 12309
e-mail: knobloch@research.ge.com

Chris Kapusta
General Electric Global Research,
One Research Circle,
Niskayuna, NY 12309
e-mail: kapusta@ge.com

Jason Karp
General Electric Global Research,
One Research Circle,
Niskayuna, NY 12309
e-mail: karp@ge.com

Yuri Plotnikov
General Electric Global Research,
One Research Circle,
Niskayuna, NY 12309
e-mail: plotnikov@ge.com

Jason B. Siegel
Department of Mechanical Engineering,
University of Michigan,
1231 Beal Avenue,
Ann Arbor, MI 48109
e-mail: siegeljb@umich.edu

Anna G. Stefanopoulou
Fellow ASME
Department of Mechanical Engineering,
University of Michigan,
1231 Beal Avenue,
Ann Arbor, MI 48109
e-mail: annastef@umich.edu

Fabrication of Multimeasurand Sensor for Monitoring of a Li-Ion Battery

This paper details the fabrication and testing of a combined temperature and expansion sensor to improve state of charge (SOC) and state of health (SOH) estimation for Li-ion batteries. These sensors enable the characterization of periodic stress and strain changes in the electrode materials of Lithium-ion batteries during the charge and discharge process. These ultrathin sensors are built on a polyimide substrate which can enable direct integration between cells without compromising safety or cell cooling design. Leveraging the sensor design and fabrication process used to create inductive coil eddy current (EC) sensors for crack detection, these sensors were characterized on three Panasonic 5 A-h cells showing the capability to measure expansion of Li-ion batteries. By sensing the intercalation effects, which cause cell expansion, improvements in estimation of SOH and SOC can be enabled through the use of physics-based battery models, which combine the thermal, mechanical, and electrochemical aspects of its operation.
[DOI: 10.1115/1.4039861]

Introduction

Li-ion batteries are ubiquitous in consumer electronics applications due to their high energy density, high power density, low cost, and reliability. However, the use of Li-ion batteries for automotive applications is currently limited due to gaps in safety, durability, and cost in comparison to the operating requirements and market demands. One key area for improvement in the design of battery systems lies in battery state estimation [1]. These estimates of battery states determine the operating limits of the battery, which directly impact the size and cost of Li-ion battery systems. It is estimated that overly conservative operating limits used by battery management systems (BMS) lead to battery packs that are 1.25-2x larger and more expensive than packs that are sized appropriately to their use conditions. Today's battery systems for automotive applications utilize voltage, current, and selected temperature measurements to inform equivalent circuit models and estimates of the state of charge (SOC) and state of health (SOH). This is primarily driven by the low computational complexity of the equivalent circuit models and minimization of sensing cost. However, the combination of limited measurement capability and models without the coupled mechanical, electrochemical, and thermal physics lead to unrealized battery performance.

Battery expansion is a measurement parameter with the potential to provide new insight and information into battery operation. The intercalation of Li ions into and out of the battery electrodes causes expansion of the cells [2], and the resulting force can be measured when the cells are constrained in a battery pack. Several methods have been used to characterize battery expansion and used to understand SOH and SOC. Electrodes mapped with digital image correlation show that electrode porosity is directly related to strain fields generated in the electrodes [3]. Neutron transmission imaging of a pouch cell was used to determine the battery operating and design factors such as C-rate (the rate at which a battery is charged or discharged), pack compression, and electrode chemistry impact on SOH [4]. Pack compression has been found to have a strong effect on capacity drop of pouch cells resulting in rapid performance degradation due to permanent electrode volume changes [5]. In both Refs. [4] and [5], an increase in cell thickness (noncyclable) with aging has been shown and is correlated with capacity loss. A thickness changes up to 4% of the total cell thickness during Li intercalation in LG pouch cells under constant loading was observed in Ref. [6]. For hard cased cells, a 1.5% thickness change was observed with displacement sensors over the entire SOC range with a strong dependence of contraction on the C-rate during discharge

[1]Corresponding author.

Contributed by the Electronic and Photonic Packaging Division of ASME for publication in the Journal of Electronic Packaging. Manuscript received June 7, 2017; final manuscript received March 27, 2018; published online May 11, 2018. Assoc. Editor: Kaustubh Nagarkar.

[7]. However, the techniques detailed here are generally limited to characterization in a laboratory setting and not feasible for implementation in automotive applications.

Recently, new models and state estimation techniques have been developed based on the enhanced observability enabled by expansion measurements. One technique is to augment voltage measurements with expansion or force measurements to improve estimation of SOC [8,9]. Another example is an incremental capacity analysis using the combination of voltage and force measurements, which was shown to be correlated with capacity loss [10]. However, practical implementation of these techniques requires the development of low-cost sensors that can be located within the limited confines of the battery pack. Thin temperature sensors integrated between cells in a pack in the high-temperature areas can enable new battery model parameterization and pack modeling techniques [11].

This paper presents a multimeasurand sensor platform combining temperature and battery expansion measurement integrated into automotive hybrid electric vehicle pack. Based on a Kapton substrate and thin film processing, the ultrathin sensor system was inserted between cells in the pack without causing battery degradation or failure and enabled observations of battery mechanics not possible with existing sensors. Details of the fabrication and integration process will be discussed along with laboratory results showing its performance in measuring temperature and battery expansion.

Sensor Integration

Figure 1 shows an example of a Li-ion battery pack used in the Model Year 2014 Hybrid Electric Ford Focus. The battery pack consists of two arrays, each containing 38 5 A-h Nickel Manganese Cobalt oxide/graphite Li-ion cells, which are connected in series and compressed between aluminum end plates. A black plastic spacer, shown in Fig. 1, between cells provides partial contact to the adjacent cells and allows airflow between cells for cooing and to help maintain a uniform temperature. Temperature profiles across the surface of the cell are less than 1 °C, due to the high thermal conductivity of the aluminum cell casing and internal structure shown in Ref. [11]. In this application, the cells are cooled with vehicle cabin air conditioned by the vehicle. Air flows from the fan through and underneath the front string to reach the rear string [11]. The cooling air should be regulated between 0 °C and 30 °C, to maintain cell temperatures below 60 °C. The compression force is estimated to be on the order of 900 N (200 lbs), depending on the SOC of the battery, which is high enough to physically deform the exterior of the cell casing. Rectangular depressions aligning with points of contact with the plastic spacer can be seen on the cell when disassembling the pack. The deformation of the cell casing into the air channel was modeled in Ref. [12].

In the existing pack configuration, current, voltage, and selected temperature measurements are used to inform Ford's proprietary battery control scheme. Ten thermistors mounted to the top of select cells between the electrodes provide a limited view of the thermal profile within the pack. These sensors are over 1 mm thick and therefore are not suitable for mounting to the cell face. The temperature sensor output is communicated to the BMS and used to estimate the core cell temperature, which is used as one of the limits on battery performance. Thermal models of these cells have shown that the highest temperatures are on the surface of the cells rather than the top where the sensor is located [11]. Direct measurement of the highest temperature regions of the cell would

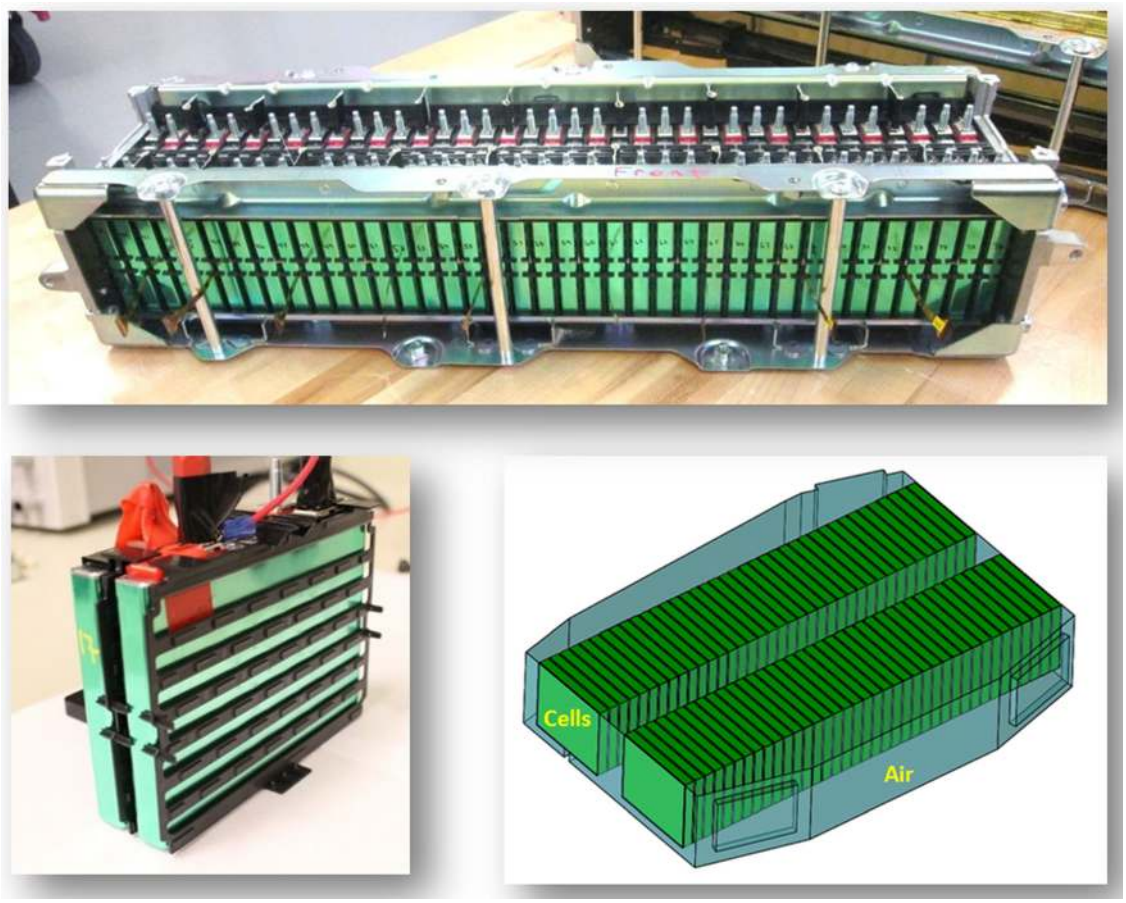

Fig. 1 Lower right: In the Ford Fusion 2014 Model Year hybrid electric vehicle pack, 76 5 A-h cells are configured into two strings with active air cooling. Top: An example of a single string where air flows between the cells. Lower left: A two-cell portion of the pack showing the plastic spacers, which allow air flow between the cells for cooling.

enable more accurate estimates of internal battery core temperatures, which are difficult to measure outside of the laboratory [13]. This information would result in increased battery utilization through reducing operating margins in the battery pack design by eliminating uncertainty.

Based on the cell and pack configuration, there is limited space to integrate sensors for either temperature or expansion on the front faces of the cells. The plastic spacers are approximately 1.5 mm thick, which limits any sensor solution to thicknesses that will minimize obstruction and impact on cooling air flow between the cells. In addition, wiring and sensor count should be minimized when possible to improve the cost position of the solution. Therefore, the objective of the multimeasurand sensor platform is to develop a thin sensor that can enable expansion measurements between cells and temperature measurements on the front faces of the cell where the temperature is more representative of the core. To allow for the integration of multiple measurements on the same flexible substrate, Kapton or polyimide was chosen as the substrate material, which leverages General Electric's experience in flex-based packaging for electronics packaging and the utilization of thin film processes.

Temperature Sensor Design. There are many established methods for temperature measurement including thermocouples, thermistors, and resistance temperature detectors (RTDs) that were considered. For this application, RTDs were chosen due to several key factors. First, thin film RTDs are a well-established commercial product with understood behavior. Second, a Platinum (Pt) RTD is compatible with the thin film processes available at GE and it has a stable and linear resistance–temperature relationship over a wide temperature range. Typically, Platinum RTDs are manufactured on rigid ceramic and are typically designed to meet a nominal resistance of around 100 Ω. By targeting the same resistance, the sensor could utilize existing mass-produced analog signal conditioning circuitry for measuring temperature.

Figure 2 shows several element designs for a 100 Ω Platinum RTD. A serpentine structure and two types of straight elements, ac shape, and a linear element design, were explored for the sensor. Testing with prototypes showed no discernable difference between the performances. The straight element design was chosen due to its simpler design with smaller area that would reduce potential strain cross-sensitivity.

Expansion Sensor Design. Given the space constraints of the pack installation, a new technology for cell expansion measurement was needed. GE had previously developed a flat coil eddy current (EC) sensor, which leveraged the manufacturing processes of electronic packaging for the inspection of jet engines [14] and initial results for the measurement of cell expansion was reported [15]. The design of this sensor allows for the integration of the temperature sensor manufacturing process with that of the eddy current sensor.

The expansion sensor operates via the generation of eddy currents in a conductive material adjacent to a coil, which is excited by alternating current [16]. Electromagnetic coupling to the conductive casing generates an opposing magnetic field that influences the impedance of the coil, which is measured by the readout electronics. In the battery application, the sensor would be attached directly to the front face of the Li-ion cell and measure the gap change between two adjacent cells. The hard cell Panasonic batteries use a thin aluminum outer package, which serves as the conductive material in the sensor operation. This approach is also applicable for soft-sided pouch cells as the metalized Mylar laminate forming the pouch had comparable conductive properties. It should be noted that the skin depth of our sensor is approximately 60 μm, which is thicker than the cell wall so there may be some influence of the material within the cell.

Direct placement of the coil on the conductive cell case would fully saturate the coil response and obscure any change from the adjacent cell wall. This effect was eliminated through two specific features of the coil design. First, since the response of the sensor is inversely proportional to the distance from the conductive plane, the output range of the flat coil EC sensor was optimized in the regime between 0 mm and 1 mm such that metal more than 1 mm away had a minimal effect on the sensor output. Since the gap between cells is approximately 1.5 mm, a ceramic standoff of thickness 1 mm was attached to the back of the coil to move it away from the proximate cell wall and locate the coil in the most sensitive portion of the response from the adjacent cell. Thus, in this configuration, the response of the coil would be a function of the gap between the cells due to the combination of the adjacent cell wall moving in closer proximity to the coil due to cell swelling and the motion generated by the coil itself due to the underlying cell swelling. In a final production product, one could envision the ceramic standoff made as part of the spacer, for easier integration into the pack.

Figure 3 shows an image of the coil. The coils were composed of 50 μm line/50 μm pitch Copper with 20 turns around a diameter of 3 mm. The traces leading to the coil were 250 μm wide Copper with a ground plane underneath. Coils were excited with a 2 MHz square wave and had impedances of 9.8 Ω and 1.09 μH.

Sensor Platform Fabrication

The fabrication process for the multimeasurand sensor platform is shown in Fig. 4. A Kapton substrate of 25 μm in thickness is laminated onto a 9 in processing frame to aid in handling thru the process. First, the Platinum RTDs for temperature sensing is formed on the substrate. This is done through a liftoff process using AZ photoresist, to define the sensor shape and evaporation of approximately 2000 Å of Platinum on the front side of the substrate. Once the photoresist is removed, vias are formed using an ESI 5330 UV laser system. The vias are through holes in the Kapton substrate, which will provide interconnect between the front side and the backside of the substrate for the coils. These vias are aligned to the Pt layer that was previously deposited. A Ti/Cu/Ti set of metal layers is blanket deposited on both sides of the substrate to form the eddy current coils, interconnect to the RTDs and to route to the connectors. This is accomplished through sputtering of 2000 Å Ti and 6000 Å Cu then subsequently plating 4 μm of Cu and then sputtering 1000 Å of Ti. Ni/Au pads are plated up

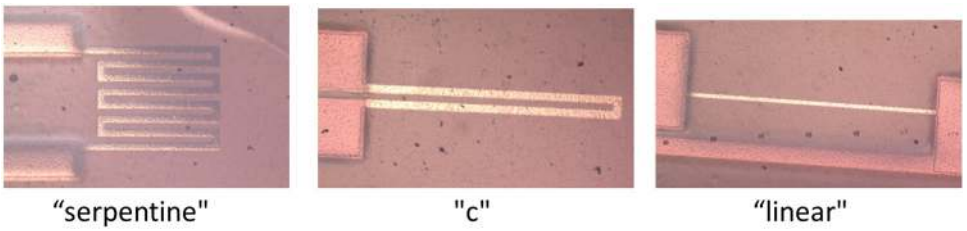

Fig. 2 Three different Pt RTD designs were considered for the sensor platform. Images above show test structures of Pt on Kapton that were tested for temperature sensitivity and performance.

Fig. 3 Image of the eddy current expansion sensor utilizing a flat coil design implemented with Cu traces on a Kapton film

to form a reliable connection to the Ziff–connector interface, with thicknesses of 1 μm of Ni and 1500 Å of Au. Photolithography processes are performed to define the pattern in photoresist, and the metal stack is wet etched to pattern the eddy current coils, the ground plane, and the terminations. Dilute HF was used to etch the Ti and a $FeCl_2$ solution was used to etch the Copper. After etching and removal of the resist, the circuit was laminated on both sides with a 25 μm thick coverlay (0.5 mil adhesive/0.5 mil Kapton) to encapsulate the metal lines and protect against shorting to the metal case of the battery. The end terminations were designed so that the sensor can be connected to a Ziff connector at the edge of the flex. The Kapton at the edge of the flex was removed so that the Au is accessible for the Ziff connector. Figure 5 shows an example of the final sensor after being singulated from the frame using a laser. Individual sensors were fitted with 1 mm thick ceramic spacers underneath the eddy current coil to offset the measurement gap. These spacers were hand aligned and attached with an epoxy for the prototype but could be automated in the future.

Prior to testing and installation, each sensor required calibration for temperature and expansion measurement. For temperature, the sensors were immersed in a temperature controlled bath at five set points between −20 °C and 60 °C. From these tests, a linear relationship between temperature and resistance was determined. A specific setup was developed to calibrate the individual eddy current sensors after the temperature sensor calibration was completed. This calibration was performed using a precision translation stage to vary the gap to the target material. Gap calibrations were collected at multiple temperature levels to derive transfer functions for each sensor as detailed in Ref. [17].

Pack Integration and Measurement Locations. For initial characterization of temperature in a pack and to minimize the volume of wires needed for the harness, three RTDs were placed along the length of the Kapton, which would allow measurement of the spatial temperature gradient. Figure 6 shows the orientation of the sensor with respect to the battery. In this configuration, the eddy current sensor was positioned in the center of the battery where the expansion is the maximum. The sensors were attached to the battery using a silver filled epoxy underneath the coil and the three RTDs. This epoxy was used to ensure a good thermal connection to the battery for the RTDs. Sensor attachment was reinforced with Kapton tape across the top of the sensor except in the area of the eddy current coil. A new pack was dissembled and sensors were mounted on every fourth cell. The pack was then reassembled and tightened to the specified compression level. The completed pack including 18 mounted sensors is shown in the

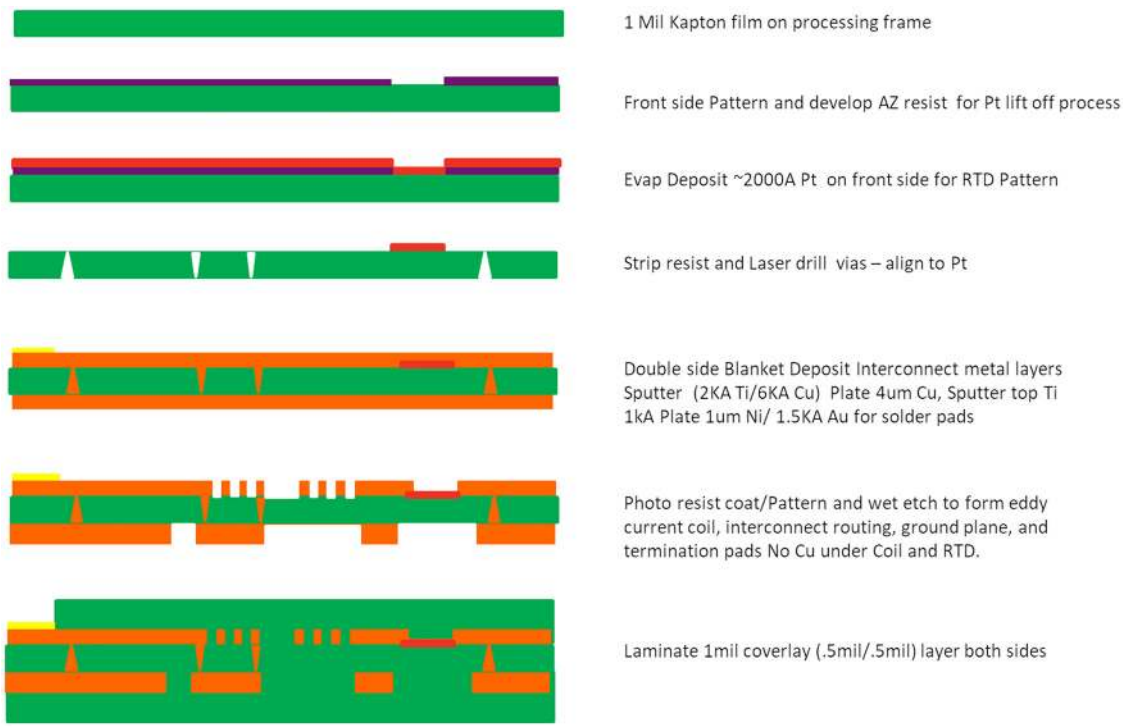

Fig. 4 Fabrication process flow for the sensor platform

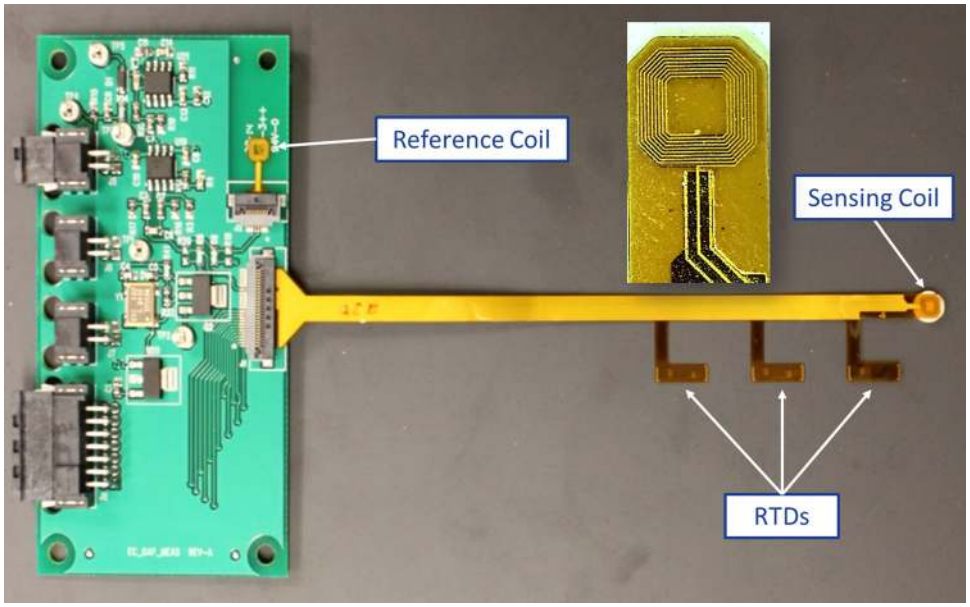

Fig. 5 An example of the fabricated sensor with the associated electronics. Each sensor is composed of three Platinum RTDs and one eddy current expansion sensor. The electronics primary function is to drive and read the eddy current sensor as well as send the sensor output to the data acquisition system.

upper image of Fig. 1, with the flexible leads protruding past the frame.

For integration into the pack, a mounting rail was designed to hold the sensor electronics board required to operate the eddy current sensor and transmit signals to the data acquisition system. Figure 7 shows one of the strings with the rail with several unpopulated boards hung from the top of the rail. The boards were oriented such that their cross section was minimized and allow

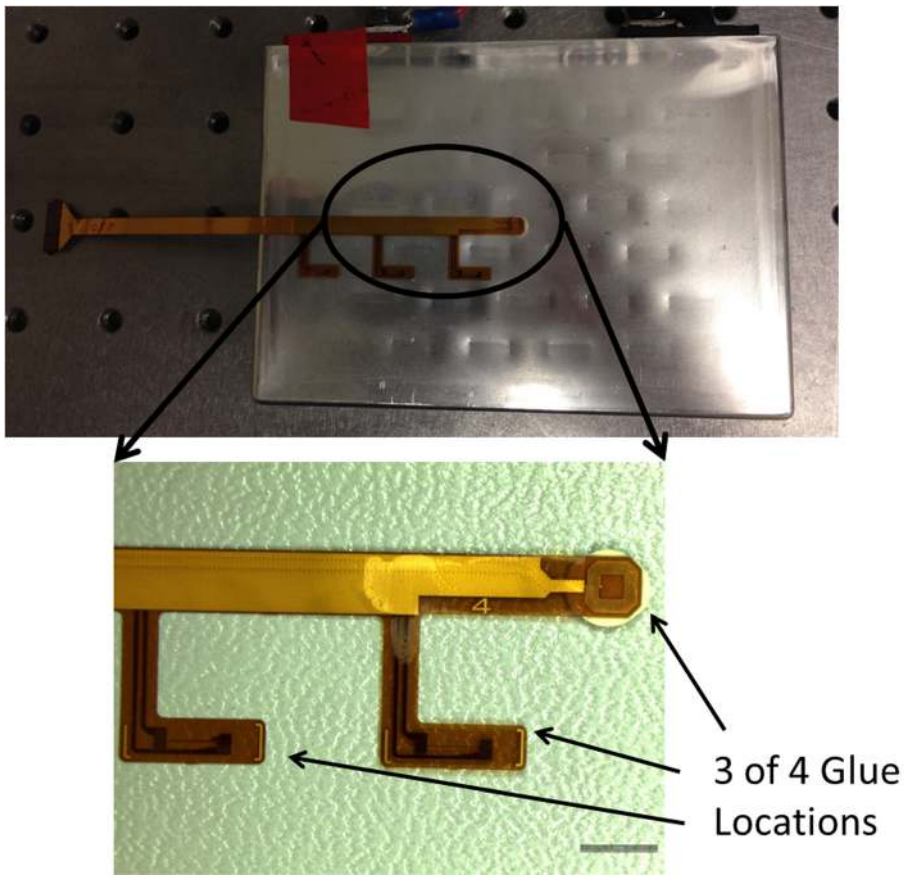

Fig. 6 The sensor was positioned on the 5 A-h cell and attached directly to the surface using a silver epoxy underneath the temperature and eddy current elements (scale bar indicates 1 cm)

Fig. 7 A rail (shown in black) was designed to hold the electronics needed for the sensors. The boards were oriented to allow flow through to the cells.

airflow to reach the cells for cooling. In production, it is envisioned that the sensors could be routed to the top of the pack and connect to the existing interface board, and eliminate this airflow concern. Pack thermal models were created based on the work in Ref. [11] in order to understand the impact of the flow obstruction on the temperature distribution. These models were validated and adjusted prior to testing based on data from the baseline temperature sensors used in the pack.

The intention of this test was to utilize more sensors than would be envisioned for a commercial implementation of the system, to provide additional measurements for model validation. Based on the results of these tests, the minimum number and location of sensors can be determined using a model of the pack temperature distribution. Sensor placement is a critical issue since overall system cost depends on the number of sensors. However, to keep costs down, manufacturers would like to minimize or reduce the number of sensors. There has been prior work on temperature sensor placement in large air-cooled packs [18]. The number of sensors boards (19) and sensors per board (4) drove a complex and large wire assembly for these tests. This can be seen in the fully assembled pack shown in Fig. 8. In practical applications, the temperature sensors could easily be multiplexed to reduce lead-out wiring.

Three-Cell Validation. Testing of the free expansion for single cells, without the forces imposed by the packaging of the string, was performed with early prototypes of the eddy current sensor [15] showing 100 μm of expansion across the full state of charge range. Other preliminary testing indicated that the pack assembly force has a significant impact on the expected expansion measured by the sensor. Prior to the implementation of the sensor on a full pack, testing was performed in a three-cell validation rig at the University of Michigan to understand the expansion sensor output and behavior as well as supply early data to derive and validate the algorithm and models that would be implemented on the Ford Fusion pack. Figure 9 shows an image of the sensor integrated on the middle cell of a three-cell rig, which emulates the pack prestress. A compressive fixture with Garolite end plates was built to hold the cells on either side. Four washer type load cells (Omega LC8125-250-100) were mounted on the cross bolts of the fixture to examine the force behavior of the cells during operation. The pack was assembled utilizing the force specifications applied in the assembly of the commercial packs of 250 lbs and measured using the load washers.

The three-cell rig was placed in a temperature-controlled chamber (Cincinnati Sub Zero), which maintained the temperature of the fixture at ambient conditions (25–26 °C) and can allow future testing of the sensor system operating at temperature conditions corresponding to hot summer or cold winter environments. Figure 10 shows a 1C charge–discharge starting from 50% state of charge. Following the discharge, the battery was recharged and discharged at the 4 h rate. The chamber temperature was maintained at 25 °C, and the cell temperature rose by less than 1 deg

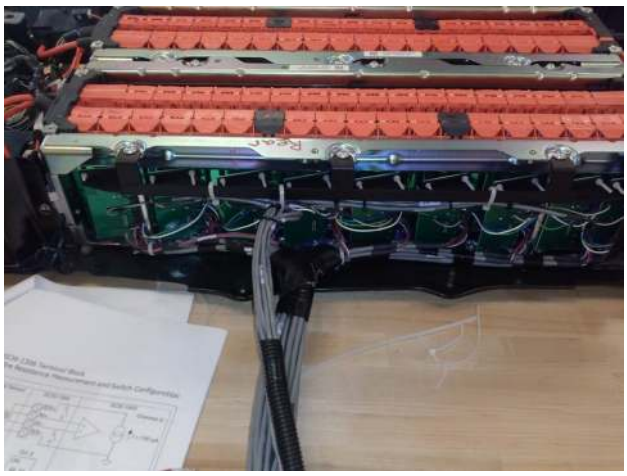

Fig. 8 A fully assembled pack with sensors and electronics highlighting the large number of wires required for operation (four wires per sensing element)

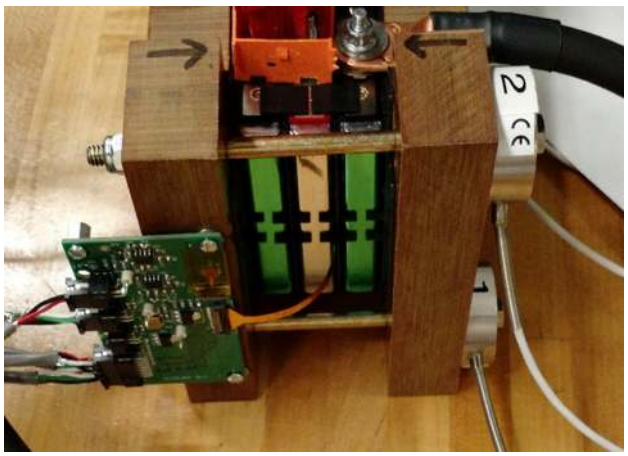

Fig. 9 A three-cell test rig, which replicates the pack conditions, was used to understand and quantify sensor performance

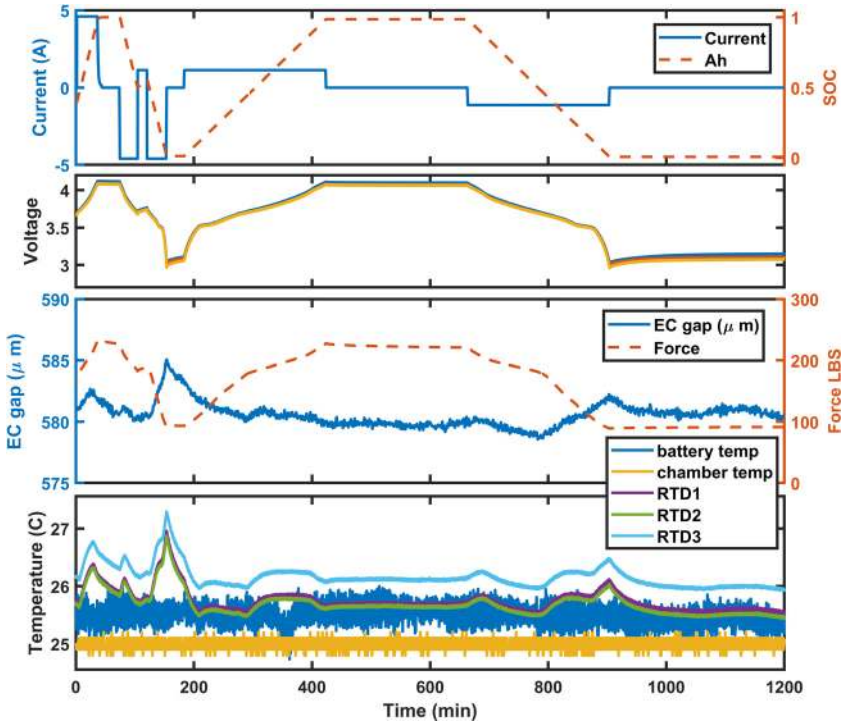

Fig. 10 Test data showing the temperature, expansion, and force in a three-cell test rig replicating pack conditions during charge and discharge

during the 1C discharge and less than 0.25 °C during the C/4 discharge. In addition to the characteristics of the test, Fig. 10 shows the data for temperature, expansion, and force for this test. The RTD sensors followed the perturbations of temperature, which were a result of heating of the battery during discharge and which were not measured by the thermistors used in the Ford BMS. The noise level of the RTDs was lower than these thermistor (labeled battery temp). There is very little temperature change in the cells because the C-rate is low.

The assembly force of the pack has a significant impact on the expansion measurement of the eddy current sensor due to the hard-cased aluminum package and rigid plastic spacer. A detailed three-dimensional finite element model of the cells was generated to study the relationship between electrode volume change due to lithium intercalation and deformation of the cell casing into the air channels [12], which is measured by the sensor. Although not the focus of this paper, the initial preloading can be estimated using the model as shown in Ref. [12], changes in preload could be related to nonrecoverable swelling of the battery electrodes due to aging, such as SEI growth. The total expansion during the test was approximately 6 μm, 16 times less than the free expansion of the battery. The response of the sensor for these small increments of SOC at high to mid SOC is indistinguishable from the noise with most of the response at the low SOC range (less than 30%). The sensor also appears to be affected by the temperature of the cell with oscillation of the response when the cell is discharged. This contrasts with the response of the force. The change in force on the pack is very significant through the range of SOC tested with about 250 lbs total dynamic range. The graph also confirms what was seen in the expansion that the majority of the force change is in the lower portion of the SOC range with lower rate of change in force with SOC around 50% SOC.

The limitations of the sensor for hard encased cells due to the specific packaging, with rigid spacers, limited the deformation of the cell and hence the effectiveness of the eddy current displacement sensor in the demonstrated application. For pouch cells packaged with compliant foam pads, the cells are permitted to have a larger expansion, which is easier to measure for the sensors presented here. In addition to the specific packaging effects, the material chemistry and stoichiometric ratio of anode and cathode active materials are important for the overall measurement since the overall cell swelling is the sum of the anode (expansion) and the cathode (contraction) during charging. Tests with a Lithium Iron Phosphate pouch cells are presented in Ref. [19].

Conclusions

A sensor platform has been developed to measure temperature and expansion of Li-ion batteries in order to better inform battery models and improve pack performance through new methods of estimation of state of health and state of charge. For the measurement of temperature, a platinum RTD was designed and integrated into the same Kapton substrate as a flat coil eddy current sensor used for the measurement of expansion. The total thickness of the sensor is less than 100 μm. The sensors were designed for integration into a 2014 Model Year Ford Focus battery pack. The sensor was integrated into a three-cell fixture to understand the performance in pack-like environment and operation. The RTD performance exceeded the noise performance and sensitivity of the existing thermistor and was able to detect small changes in the battery temperature due to heat from discharging. Deflections of the battery over the full scale of SOC was 6 μm near the noise and sensitivity limits of the sensor with most of the deflection in the lower 30% of SOC. Future testing is planned for a full pack over a range of operating temperatures and drive cycles. These tests will be used to validate the ability of the improved sensing and battery models to enable adaptive, physics-based battery control to improve battery utilization and decrease system cost.

Acknowledgment

The authors would like to thank the work and collaboration of their partners from University of Michigan including Dr. Bogdan Epureanu as well as Dyche Anderson and Arnold Mensah-Brown from Ford Motor Company. The authors would also like to acknowledge the Global Research Center's cleanroom staff for

their contributions to fabricate the sensors. Brian Engle from Amphenol Advanced Sensors provided invaluable consultation and advice throughout the project. The information, data, or work presented herein was funded in part by an agency of the United States Government. Neither the United States Government nor any agency thereof, nor any of their employees, makes any warranty, express or implied, or assumes any legal liability or responsibility for the accuracy, completeness, or usefulness of any information, apparatus, product, or process disclosed, or represents that its use would not infringe privately owned rights. Reference herein to any specific commercial product, process, or service by trade name, trademark, manufacturer, or otherwise does not necessarily constitute or imply its endorsement, recommendation, or favoring by the United States Government or any agency thereof. The views and opinions of authors expressed herein do not necessarily state or reflect those of the United States Government or any agency thereof.

Funding Data

- The information, data, or work presented herein was funded in part by the Advanced Research Projects Agency-Energy (ARPA-E), U.S. Department of Energy, under Award No. DE-AR0000269.
- Amphenol Advanced Sensors.

References

[1] Lu, L., Han, X., Li, J., Hua, J., and Ouyang, M., 2013, "A Review on the Key Issues for Lithium-Ion Battery Management in Electric Vehicles," J. Power Sources, **226**, pp. 272–288.

[2] Sethuraman, V., Van Winkle, N., Abraham, D., Bower, A., and Guduru, P., 2012, "Real-Time Stress Measurements in Lithium-Ion Battery Negative-Electrodes," J. Power Sources, **206**, pp. 334–342.

[3] Qi, Y., and Harris, S. J., 2010, "In Situ Observation of Strains During Lithiation of a Graphite Electrode," J. Electrochem. Soc., **157**(6), pp. A741–A747.

[4] Siegel, J. B., Stefanopoulou, A. G., Hagan, P., Ding, Y., and Gorsich, D., 2013, "Expansion of Lithium Ion Pouch Cell Batteries: Observations From Neutron Imaging," J. Electrochem. Soc., **160**(8), pp. A1031–A1038.

[5] Cannarella, J., and Arnold, C. B., 2014, "Stress Evolution and Capacity Fade in Constrained Lithium-Ion Pouch Cells," J. Power Sources, **245**, pp. 745–751.

[6] Lee, J. H., Lee, H. M., and Ahn, S., 2003, "Battery Dimensional Changes Occurring During Charge/Discharge Cycles—Thin Rectangular Lithium Ion and Polymer Cells," J. Power Sources, **119–121**, pp. 833–837.

[7] Oh, K.-Y., Siegela, J. B., Secondo, L., Ung Kim, S., Samada, N. A., Qin, J., Anderson, D., Garikipati, K., Knobloch, A., Epureanu, B. I., Monroe, C. W., and Stefanopoulou, A., 2014, "Rate Dependence of Swelling in Lithium-Ion Cells," J. Power Sources, **267**, pp. 197–202.

[8] Kim, Y., Samad, N. A., Oh, K. Y., Siegel, J. B., Epureanu, B. I., and Stefanopoulou, A. G., 2016, "Estimating State-of-Charge Imbalance of Batteries Using Force Measurements," American Control Conference (ACC), Boston, MA, July 6–8, pp. 1500–1505.

[9] Mohan, S., Kim, Y., Siegel, J. B., Samad, N. A., and Stefanopoulou, A. G., 2014, "A Phenomenological Model of Bulk Force in a Li-Ion Battery Pack and Its Application to State of Charge Estimation," J. Electrochem. Soc., **161**(14), pp. A2222–A2231.

[10] Samad, N. A., Kim, Y., Siegel, J. B., and Stefanopoulou, A. G., 2016, "Battery Capacity Fading Estimation Using a Force-Based Incremental Capacity Analysis," J. Electrochem. Soc., **163**(8), pp. A1584–A1594.

[11] Samad, N. A., Wang, B., Siegel, J. B., and Stefanopoulou, A. G., 2017, "Parameterization of Battery Electro-Thermal Models Coupled With Finite Element Flow Models for Cooling," ASME J. Dyn. Syst., Meas. Control, **139**(7), p. 071003.

[12] Oh, K., Epureanu, B., Siegel, J., and Stephanopoulou, A., 2016, "Phenomological Force and Swelling Models for Lithium-Ion Battery Cells," J. Power Sources, **310**, pp. 118–129.

[13] Perez, H., Siegel, J., Lin, X., Stefanopoulou, A., Ding, Y., and Castanier, M., 2012, "Parameterization and Validation of an Integrated Electro-Thermal Cylindrical LFP Battery Model," ASME Paper No. DSCC2012-MOVIC2012-8782.

[14] Plotnikov, Y., Wang, C., McKnight, W., and Suh, U., 2008, "Eddy Current Inspection of Components With Complex Geometries," Rev. Prog. QNDE, **975**(1), pp. 376–383.

[15] Plotnikov, Y., Karp, J., Knobloch, A., Kapusta, C., and Lin, Y., 2015, "Eddy Current Sensor for In-Situ Monitoring of Swelling of Li-Ion Prismatic Cells," AIP Conf. Proc., **1650**, pp. 434–442.

[16] Knobloch, A., Karp, J., Plotnikov, Y., Kapusta, C., Siegel, J., Samad, N., and Stefanopoulou, A., 2017, "Novel Thin Temperature and Expansion Sensors for Li-Ion Battery Monitoring," IEEE Sensors, Glasgow, UK, Oct. 29–Nov. 1, pp. 1–3.

[17] Karp, J., Knobloch, A., Siegel, J., Kapusta, C., Plotnikov, Y., and Stefanopoulou, A., "Eddy Current Sensing for Expansion Measurement of Lithium-Ion Batteries," (in preparation).

[18] Lin, X., Fu, H., Perez, H. E., Siegel, J. B., Stefanopoulou, A. G., Ding, Y., and Castanier, M. P., 2013, "Parameterization and Observability Analysis of Scalable Battery Clusters for Onboard Thermal Management," Oil Gas Sci. Technol.—Rev. IFP Energies Nouvelles, **68**(1), pp. 165–178.

[19] Polóni, T., Figueroa-Santos, M. A., Siegel, J. B., and Stefanopoulou, A. G., 2018, "Integration of Non-Monotonic Cell Swelling Characteristic for State-of-Charge Estimation," American Controls Conference, Milwaukee, WI, June 27–29 (accepted).